PLOS ONE

RESEARCH ARTICLE

Statistical Determination of Rainfall-Runoff Erosivity Indices for Single Storms in the Chinese Loess Plateau

Mingguo Zheng[1]*, **Xiaoan Chen**[2]

1 Key Laboratory of Water Cycle and Related Land Surface Processes, Institute of Geographic Sciences & Natural Resources Research, Chinese Academy of Sciences, Beijing 100101, China, **2** Jiangxi Institute of Soil and Water Conservation, Nanchang 330029, China

* zhengmg.04b@igsnrr.ac.cn

Citation: Zheng M, Chen X (2015) Statistical Determination of Rainfall-Runoff Erosivity Indices for Single Storms in the Chinese Loess Plateau. PLoS ONE 10(3): e0117989. doi:10.1371/journal.pone.0117989

Academic Editor: Vanesa Magar, Centro de Investigacion Cientifica y Educacion Superior de Ensenada, MEXICO

Received: June 16, 2014

Accepted: January 6, 2015

Published: March 17, 2015

Data Availability Statement: All Data are deriven from the book "Yellow River Water Conservancy Commission, Ministry of Water Conservancy and Electric Power, PRC (1961–1971). Observed Data of Rainfall, Runoff and Sediment in the Zizhou Experimental Office over the Period 1959–1969.", which is available on application at http://loess.geodata.cn/Portal/metadata/listMetadata.jsp?category=1160. Thanks to the Data Sharing Infrastructure of Earth System Science—Data Sharing Infrastructure of Loess Plateau for providing the data.

Abstract

Correlation analysis is popular in erosion- or earth-related studies, however, few studies compare correlations on a basis of statistical testing, which should be conducted to determine the statistical significance of the observed sample difference. This study aims to statistically determine the erosivity index of single storms, which requires comparison of a large number of dependent correlations between rainfall-runoff factors and soil loss, in the Chinese Loess Plateau. Data observed at four gauging stations and five runoff experimental plots were presented. Based on the Meng's tests, which is widely used for comparing correlations between a dependent variable and a set of independent variables, two methods were proposed. The first method removes factors that are poorly correlated with soil loss from consideration in a stepwise way, while the second method performs pairwise comparisons that are adjusted using the Bonferroni correction. Among 12 rainfall factors, I_{30} (the maximum 30-minute rainfall intensity) has been suggested for use as the rainfall erosivity index, although I_{30} is equally correlated with soil loss as factors of I_{20}, EI_{10} (the product of the rainfall kinetic energy, E, and I_{10}), EI_{20} and EI_{30} are. Runoff depth (total runoff volume normalized to drainage area) is more correlated with soil loss than all other examined rainfall-runoff factors, including I_{30}, peak discharge and many combined factors. Moreover, sediment concentrations of major sediment-producing events are independent of all examined rainfall-runoff factors. As a result, introducing additional factors adds little to the prediction accuracy of the single factor of runoff depth. Hence, runoff depth should be the best erosivity index at scales from plots to watersheds. Our findings can facilitate predictions of soil erosion in the Loess Plateau. Our methods provide a valuable tool while determining the predictor among a number of variables in terms of correlations.

Funding: The research is funded by the National Natural Science Foundation of China (41271306; http://www.nsfc.gov.cn/) and the Non-profit Industry Financial Program of MWR (201201083; http://www.mwr.gov.cn). The funders had no role in study design, data collection and analysis, decision to publish, or preparation of the manuscript.

Competing Interests: The authors have declared that no competing interests exist.

Introduction

Rainfall erosivity indicates the potential of a storm to erode soil. A single index of rainfall erosivity that can measure the composite effect of various rainstorm characteristics on soil erosion is highly desirable for predicting soil loss [1, 2]. It is well known that soil losses are frequently due to a few intense rainfall events [1, 3]. The most common erosivity index for single storms is the EI_{30} index (the product of the rainfall kinetic energy, E, and the maximum 30-min intensity, I_{30}), as is used in the Universal Soil Loss Equation (USLE) [4] and in the Revised Universal Soil Loss Equation (RUSLE) [5]. The calculation of EI_{30} is of high data requirements and labor intensive [2, 6]. For this reason, a large number of studies (e.g. [1, 2, 6, 7]) were devoted to developing a proxy, using more readily available data such as daily, monthly and annual precipitations, for EI_{30} and the R factor of the USLE (the mean annual total of EI_{30}).

Besides the EI_{30} index, other forms of erosivity index for storm events primarily include the $KE > 25$ index (the total kinetic energy for rainfall duration with intensity exceeding 25 mm h^{-1}) [8], the PI_m index (the product of the rainfall amount, P, and the peak rainfall intensity, I_m) [9], the I_xE_A index (the product of the excess rainfall rate, I_x, and the rainfall kinetic energy flux, E_A) [10], and the so-called A index [11]. Many local erosivity indices for single storms have also been used, such as $I15$ in Belgium [12], $EI5$ in NE Spain [13], E in Palestinian areas [14] and EI_{60} and $I60$ in Malaysia [15]. In the Chinese Loess Plateau, both *Wang* [16] and *Jia et al.* [17] suggested EI_{10} as the rainfall erosivity index; however, EI_{10} has been shown to be of similar effectiveness as EI_{30} [18]. Notably, *Chen et al.* [19] detected no significant difference among correlations between soil loss and a set of EI_t variables (EI_{10}, EI_{20}, EI_{30}, EI_{40}, EI_{50} and EI_{60}). Furthermore, it was found that EI_t did not greatly improve soil loss predictions compared with PI_t [19–21], which can thus serve as a surrogate for EI_{30}.

Both raindrops and runoff are drivers of soil erosion [22]. Runoff factors, mainly runoff volume and peak discharge, have frequently been included into an erosivity index [23–28]. The addition of runoff terms can improve the ability of models to predict soil loss or sediment yield especially for small to medium events [25, 27, 29]. Foster et al. [25] found that the lumped erosivity factors including rainfall amount, rainfall intensity and runoff amount performs better than EI_{30}, whereas erosivity factors with separate terms for rainfall and runoff erosivity performs best. However, Foster et al. [25] acknowledged their inability to determine whether the observed improvements were statistically significant or not. In the Modified Universal Soil Loss Equation (MUSLE), the EI_{30} index is replaced by a power of the product of runoff volume and peak discharge [24], as is also used in the Agricultural Policy/Environmental eXtender (APEX) model [28]. In another modified version of the USLE called the USLE-M [27], the erosivity index of single events is the product of EI_{30} and the runoff ratio. In the Loess Plateau, many studies included both terms of runoff volume and peak discharge, in a lumped or separated form, into models for predicting soil loss or sediment yield [30–32]. Nevertheless, it is well known that runoff volume alone can adequately predict sediment yield of the flood event in the Loess Plateau ($r^2 > 0.9$) [33]. A proportional model of event runoff volume and sediment yield applies well over a wide range of spatial scales from hill slopes to large-sized watersheds [34–35].

To determine the erosivity index, a large number of correlations between rainfall-runoff factors and soil loss often need to be compared (e.g. [14–17, 23, 25, 26, 36–37]). For example, the EI_{30} index was established as the rainfall erosivity index of the USLE by comparing correlations of more than 40 factors with soil loss [38–40]. As a result of the indelible sampling error, sample correlation coefficients can never be identical to population ones. Because the sample difference does not fully represent the population difference, a statistical test is needed to determine the significance of the observed sample difference. To our knowledge, no studies have applied statistical tests while determining the erosivity index with the exceptions of [12]

and [19], although a number of statistical tests for comparing dependent or independent correlations exist [41].

The object of this study is to determine erosivity indices for single storms on a statistical basis using data observed in the Chinese Loess Plateau. After describing the study area and data source, we present two methods that compare a large number of dependent correlations. The two methods build on the Meng's tests [42], which has been widely used to compare correlations in psychological research. We then determine the rainfall-runoff erosivity indices among a large number of factors using the two methods. We finally made some discussions about rainfall and runoff factors with an emphasis on the best erosivity index in the Loess Plateau.

Study Area and Data

The present study uses data observed at 5 runoff experimental plots and 4 gauging stations (Tables 1 and 2) within the Dalihe River watershed (See Fig. 1 in [35] for the location), a secondary-order river of the middle Yellow River. Typical of the Loess Plateau, the loess mantle of the Dalihe watershed is generally thicker than 100 m. The climate is typically semiarid with a mean annual precipitation of 440 mm (1960–2002). Soil erosion is primarily caused by localised short-duration, high-intensity convective rainstorms. A single storm can commonly cause a soil loss of greater than 10 000 t km^{-2}. Most of the lands were intensively cultivated with little soil conservation practices during the monitoring period (1959–1969). The terrain is very precipitous and deeply dissected.

All examined plots are located within the Tuanshangou subwatershed (latitude 37°41′N, longitude 109°58′E; See Fig. 1(c) in [35] for the location), a headwater basin of the Dalihe watershed. The plots were all under arable with crops varying between years, generally including millet, potato, mung bean, clover, sorghum and wheat. The vegetation cover rarely exceeded

Table 1. The gauging stations in the Dalihe River watershed.

Station No.[a]	Creek/River	Gauging station	Area (km^2)	Data Period	*n* [b]
3	Tuanshangou	Tuanshangou	0.18	1961–69	44
4	Shejiagou	Shejiagou	4.26	1960–69	49
9	Chabagou	Caoping	187	1959–69	64
12	Dalihe	Suide	3893	1960–69	44

[a] The station numbers correspond to those given in Fig. 1(b) in [35].

[b] *n* is the number of recorded flood events.

doi:10.1371/journal.pone.0117989.t001

Table 2. The runoff experimental plots in the Tuanshangou subwatershed.[a]

Plot	Slope length (m)	Slope (°)	Horizontal area (m^2)	Data period	*n* [b]
Plot 4	20	22	300	1963–67	25
Plot 2	40	22	600	1963–67	27
Plot 3	60	22	900	1961–69	45
Plot 7	126	32	5740	1961–69	40
Plot 9	164	27	17200	1963–69	41

[a] The layouts of the experimental plots were specified in Fig. 1(c) in [35].

[b] *n* is the number of recorded storm events.

doi:10.1371/journal.pone.0117989.t002

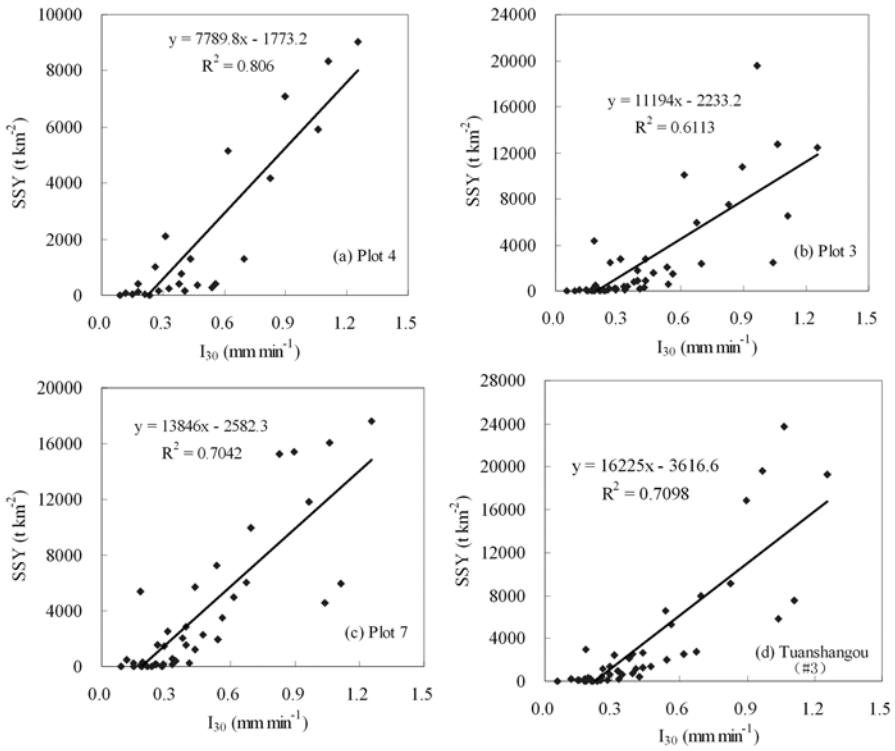

Fig 1. The relationship between I_{30} and *SSY* for the Tuanshangou station (#3) and three experimental runoff plots within it.

doi:10.1371/journal.pone.0117989.g001

25% in the plots. The recorded maximum I_{10} is 2.17 mm min^{-1} (1961–1969). Rill erosion is dominant on upland slopes. During the 1960s, the annual erosion intensity, averaging 41 000 t km^{-2} at Plots 4, 2 and 3 (Table 2), was maximized in 1966. Although rills only occurred on 5 out of 54 rainfall days, these five days contributed almost all of the annual soil loss (>96%) in 1966. Downslope, the valley side slope is generally very steep (>35°), allowing the emergence of permanent, incised gullies and mass wasting events.

Unless stated otherwise, all data used in this study were obtained from the Yellow River Water Conservancy Commission (YRWCC). The YRWCC stream-gauging crews conducted all measurements. Hyetograph data were obtained using a rainfall gauge near Plot 3 (See Fig. 1-(c) in [35] for the location). The observation interval was generally smaller than 10 min, even 1 min in many cases of high rainfall intensity. The field monitoring programs of runoff and sediment have been described in detail in [43, 44].

Based on the instantaneous measurement of water discharge and sediment concentration, the runoff depth, h (mm: total runoff volume normalized to drainage area), and the specific sediment yield, *SSY* (t km^{-2}) of single events were calculated. Conventionally, the term "soil erosion" is used for hill slopes, and the term "sediment yield" is used for a river system or watershed. For simplicity, we use *SSY* to represent both cases hereafter. The event mean sediment concentration, SC_e (kg m^{-3}) was computed by dividing *SSY* by h. The maximum instantaneous sediment concentration (SC_{max}, kg m^{-3}) was also used to represent the level of the sediment concentration of a single event.

The data we used are on a single storm basis. The runoff factors we examined include 4 factors: h, q_{max} (peak flow discharge normalised for drainage areas, m^3 s^{-1} km^{-2}), hq_{max} (the product of h and q_{max}) and h+q_{max} (the sum of h and q_{max}). The use of h+q_{max} follows [23, 30]. The

rainfall factors we examined include 12 factors: P (mm), T (rainfall duration, min), I (mean rainfall intensity, mm min^{-1}), I_{10} (mm min^{-1}), I_{20} (mm min^{-1}), I_{30} (mm min^{-1}), EI_{10}, EI_{20}, EI_{30}, PI_{10}, PI_{20} and PI_{30}. The storm kinetic energy, E (J m^{-2}), was calculated as follows:

$$E = \sum_{r=1}^{m} e_r p_r, \tag{1}$$

where e_r is the rainfall kinetic energy per unit depth of rainfall per unit area (J m^{-2} mm^{-1}), and p_r is the depth of rainfall (mm) for the rth interval among m intervals of the storm hyetograph. e_r is calculated by an empirical equation building on measurements of the drop size distribution of 195 storms in the Loess Plateau [45]:

$$e_r = 28.95 + 12.3 \log_{10} i_r, \tag{2}$$

where i_r (mm min^{-1}) represents the mean rainfall intensity for the rth interval. After unit conversion, Equation (3) is almost identical to the rainfall intensity-energy equation of the USLE [4]. The discrepancy between the two equations is less than 10% for rainfall intensities from 1 to 40 cm h^{-1}.

Methodology

Assumed that r_1 and r_2 represent the correlation coefficients of any two rainfall factors with *SSY*. To compare r_1 and r_2, *Sinzot et al.* [12] and *Chen et al.* [19] used the following statistic:

$$Z = (z_1 - z_2)\sqrt{\frac{N-3}{2}}, \tag{3}$$

where $z_1 = \frac{1}{2} ln \frac{1+r_1}{1-r_1}$ and $z_2 = \frac{1}{2} ln \frac{1+r_2}{1-r_2}$ are the Fisher z-transformed values for r_1 and r_2, N *is* the sample size. However, Equation (4) is applicable only to independent correlations [46] and cannot be used to compare r_1 and r_2 because they have a common dependent variable, *SSY*.

Meng's tests [42] are widely applied for comparing correlations between a dependent variable and a set of independent variables. This study used these tests because they take a rather simple and thus easy-to-use form and perform as well as other statistical tests in terms of controlling the Type I error and power [41]. To compare r_1 and r_2, a Z (standard normal) test (termed "Meng's Z_1 test" in the following section for simplicity) is used [42]:

$$Z = (z_1 - z_2)\sqrt{\frac{N-3}{2(1-r_x)H}}, \tag{4}$$

where r_x is the correlation between the two rainfall factors under examination,

$$H = \frac{1 - f\bar{r^2}}{1 - \bar{r^2}}, \tag{5}$$

$$f = \frac{1 - r_x}{2(1 - \bar{r^2})}, \tag{6}$$

where $\bar{r^2} = (r_1^2 + r_2^2)/2$, and f should be set to 1 if the right term of Equation (7) is larger than 1.

If the comparison involves k rainfall factors ($k > 2$), the statistic (termed "Meng's χ^2 test" hereafter) used to test the heterogeneity of the correlations of the k factors with *SSY* is as

follows [42]:

$$\chi^2(k-1) = \frac{(N-3)\sum_i (z_i - \bar{z})^2}{(1-r_x)H}, \quad (7)$$

where z_i is the Fisher z-transformed correlation coefficient for the ith rainfall factor ($i \leq k$), and $\bar{z}$ is the mean of the z_i values. In the definition of H given by Equation (5), $\bar{r^2}$ becomes the mean of the r_i^2, and r_x becomes the median intercorrelation among the factors under testing. The resulting χ^2 statistic is χ^2 distributed on k-1 degrees of freedom.

By comparing a correlation with the average of the k-1 other correlations, *Meng et al.* [42] also designed a standard Z test (termed "Meng's Z_2 test" hereafter) to determine whether a contrast exists among the k factors under examination:

$$Z = r_{\lambda z}\sqrt{\chi^2(k-1)} \quad (8)$$

where $r_{\lambda x}$ represents the correlation coefficient between z_i and λ_i. The values of λ_i are the contrast weights assigned to each z_i. The sum of the λ_is must be zero. If we wish to determine whether the first factor differs among four factors in terms of their correlations with *SSY*, for instance, λ_is should be-3, 1, 1 and 1, respectively.

Based on Meng's tests, we would use two methods to determine the rainfall-runoff erosivity indices. Method one repeatedly uses Meng's Z_2 test (Equation (8)) to remove factors that are poorly correlated with *SSY* in a stepwise way. Method two performs all paired comparisons using Meng's Z_1 test (Equation (5)). The Type I error, however, would increase when multiple comparisons are conducted simultaneously. We used Hochberg's Sharpened Bonferroni correction to counteract the problem of multiple comparisons [47, 48]. Given a p value resulting from Meng's Z_1 test, the corrected value according to the Hochberg approach is $p' = Rp$, where R is the rank value in descending order of the given p value among all obtained p values. The p values given below are one-tailed for the Meng's χ^2 test, and two-tailed for all other tests.

Using the two methods above, we would determine the rainfall erosivity index among the 12 rainfall factors and the runoff erosivity index among the 4 runoff factors. We limited our analyses of rainfall factors to the six experimental sites in the Tuanshangou subwatershed (#3 in Table 1 and the five plots in Table 2) due to the lack of reliable rainfall data at larger scale. A total of 222 events were used. Events without detailed hyetograph data were excluded. The analyses of runoff factors involve 379 events observed at all nine experimental sites listed in Tables 1 and 2.

Results

Method One—a stepwise procedure using Meng's Z_2 test

Table 3 presents the correlation coefficients between *SSY* and the 12 rainfall factors we examined. Factors other than T are generally well correlated with *SSY* ($p < 0.01$). The obtained correlation coefficients for T, I and P are much smaller than those for I_t (I_{10}, I_{20} and I_{30}), EI_t (EI_{10}, EI_{20} and EI_{30}) and PI_t (PI_{10}, PI_{20} and PI_{30}). The relationship between I_{30} and *SSY* for four of the sites was plotted in Fig. 1.

To determine whether a rainfall factor represents a contrast, we performed 12 Meng's Z_2 tests at each of the six sites in the Tuanshangou subwatershed. The result (Test 1 in Table 4) shows that the correlation coefficients of T, I and P with *SSY* are significantly smaller ($p < 0.005$) than the average of factors other than itself at every site. Factors of PI_{20} and PI_{30} are not contrasts ($p > 0.05$) at any site. Hence, these five factors (T, I, P, PI_{20} and PI_{30}) were excluded as candidates for the erosivity index. Meng's Z_2 tests of the seven remaining factors shows that

Table 3. Correlation coefficients of the rainfall factors with *SSY* and SC_e.[a]

	SSY						SC_e [b]					
	Plot 4	Plot 2	Plot 3	Plot 7	Plot 9	#3	Plot 4	Plot 2	Plot 3	Plot 7	Plot9	#3
I_{10}	**0.84**	**0.82**	**0.80**	**0.75**	**0.78**	**0.76**	0.44	0.16	0.23	0.35	0.39	**0.71**
I_{20}	**0.89**	**0.88**	**0.80**	**0.81**	**0.82**	**0.82**	0.38	0.16	0.12	0.28	0.35	**0.62**
I_{30}	**0.90**	**0.90**	**0.78**	**0.84**	**0.84**	**0.84**	0.32	0.09	0.02	0.16	0.25	0.44
EI_{10}	**0.90**	**0.88**	**0.81**	**0.83**	**0.88**	**0.86**	0.19	0.04	0.12	0.18	0.20	0.37
EI_{20}	**0.90**	**0.88**	**0.78**	**0.83**	**0.87**	**0.87**	0.17	0.02	0.08	0.13	0.17	0.30
EI_{30}	**0.88**	**0.87**	**0.75**	**0.83**	**0.86**	**0.86**	0.12	-0.04	0.02	0.04	0.09	0.17
PI_{10}	**0.81**	**0.82**	**0.75**	**0.81**	**0.84**	**0.82**	0.04	-0.04	0.10	0.16	0.14	0.24
PI_{20}	**0.81**	**0.82**	**0.73**	**0.80**	**0.84**	**0.82**	0.03	-0.05	0.06	0.11	0.11	0.17
PI_{30}	**0.79**	**0.81**	**0.69**	**0.80**	**0.82**	**0.81**	-0.01	-0.10	0.00	0.03	0.04	0.05
T	-0.13	-0.03	-0.01	0.02	0.00	-0.03	-0.48	-0.11	-0.02	-0.14	-0.15	-0.38
I	0.29	0.25	**0.55**	**0.40**	**0.55**	**0.50**	0.41	-0.03	0.10	0.30	0.27	0.50
P	**0.48**	**0.53**	**0.46**	**0.55**	**0.61**	**0.54**	-0.26	-0.18	-0.01	-0.01	-0.03	-0.15

[a] Boldface denotes statistical significance at the 0.05 level. Meanings and units of the variables were specified in Section "Study area and data." The same is for other tables.

[b] Only major sediment-producing events were used to calculate the correlation coefficients.

doi:10.1371/journal.pone.0117989.t003

Table 4. *p* values resulting from Method One for the rainfall factors.[a]

Test[b]	Site	I_{10}	I_{20}	I_{30}	EI_{10}	EI_{20}	EI_{30}	PI_{10}	PI_{20}	PI_{30}	*T*	*I*	*P*
1	Plot 4	0.12	**	**	**	**	**	0.46	0.44	0.76	**	**	**
	Plot 2	0.22	**	**	**	**	**	0.33	0.27	0.45	**	**	**
	Plot 3	**	**	**0.02**	**	**0.02**	0.15	0.14	0.44	0.94	**	**	**
	Plot 7	0.71	0.05	**	**	**	**	0.07	0.07	0.12	**	**	**
	Plot 9	0.94	0.12	**0.02**	**	**	**	**0.03**	0.05	0.13	**	**	**
	#3	0.87	0.07	**0.01**	**	**	**	0.09	0.07	0.12	**	**	**
2	Plot 4	0.16	0.75	0.38	0.25	0.24	0.81	**0.02**					
	Plot 2	0.12	0.67	0.12	0.58	0.48	0.86	0.06					
	Plot 3	0.46	0.40	0.90	0.24	1.00	0.18	0.20					
	Plot 7	**0.01**	0.76	0.30	0.51	0.41	0.46	0.62					
	Plot 9	**	0.33	0.92	0.10	0.15	0.33	0.87					
	#3	**	0.41	0.80	0.15	0.08	0.17	0.34					
3	Plot 4		0.67	0.90	0.69	0.69	0.62						
	Plot 2		0.80	0.38	0.89	0.98	0.61						
	Plot 3		0.41	0.79	0.23	0.90	0.11						
	Plot 7		0.33	0.62	0.94	0.80	0.87						
	Plot 9		0.08	0.44	0.25	0.36	0.68						
	#3		0.08	0.56	0.49	0.31	0.54						

[a] Each *p* value corresponds to a Meng's Z_2 test and indicates whether the factor under examination can be considered as a contrast.

** denotes statistical significance at the 0.01 level. Boldface denotes statistical significance at the 0.05 level.

[b] Test 1 involves all 12 factors we examined, Test 2 involves seven and Test 3 involves five of the factors. See Section "Method One" for details.

doi:10.1371/journal.pone.0117989.t004

Table 5. Correlation coefficients of the runoff factors with *SSY* and SC_e.[a]

Site	*SSY*				SC_e[b]			
	h	q_{max}	$h+q_{max}$	hq_{max}	h	q_{max}	$h+q_{max}$	hq_{max}
Plot 4	**0.94**	**0.96**	**0.96**	**0.92**	0.33	0.41	0.39	0.26
Plot 2	**0.96**	**0.86**	**0.92**	**0.91**	-0.002	0.35	0.26	-0.06
Plot 3	**0.94**	**0.91**	**0.95**	**0.95**	0.04	0.21	0.17	0.21
Plot 7	**0.99**	**0.89**	**0.95**	**0.89**	-0.19	0.02	-0.06	-0.24
Plot 9	**0.99**	**0.9**	**0.96**	**0.91**	0.04	0.23	0.18	0.18
#3	**0.99**	**0.92**	**0.97**	**0.93**	0.22	**0.63**	**0.52**	0.44
#4	**0.99**	**0.92**	**0.99**	**0.95**	0.35	**0.55**	**0.45**	**0.41**
#9	**0.99**	**0.91**	**0.99**	**0.91**	0.20	0.30	0.22	0.20
#12	**0.97**	**0.84**	**0.98**	**0.94**	-0.07	0.24	-0.07	0.08

[a] Boldface denotes statistical significance at the 0.05 level.

[b] Only major sediment-producing events were used to calculate the correlation coefficients.

doi:10.1371/journal.pone.0117989.t005

PI_{10} at Plot 4 and I_{10} at Plot 7, Plot 9 and #3 are less correlated with *SSY* (Test 2 in Table 4; $p < 0.02$). When factors of I_{10} and PI_{10} were removed (Test 3 in Table 4), no contrast was detected among the five remaining factors of I_{20}, I_{30}, EI_{10}, EI_{20} and EI_{30} at all sites ($p > 0.08$). The same result holds when using Meng's χ^2 test, which returns a quite high p value at the six sites (0.96, 0.92, 0.43, 0.90, 0.31 and 0.39, respectively), to examine the heterogeneity of the correlations of the five factors with *SSY*.

The four runoff factors of h, q_{max}, $h+q_{max}$ and hq_{max} are all highly correlated with *SSY* ($p < 0.01$) at all nine sites, from plots to watersheds (Table 5). The derived correlation coefficients between h and *SSY* are either at the maximum or simply slightly smaller than the maximum (generally < 0.01) at each site. Meng's Z_2 tests (Table 6) show that the correlation between h and *SSY* is significantly higher than the average of the three remaining factors at seven of nine examined sites ($p < 0.0006$). In contrast, the correlation between q_{max} and *SSY* is significantly lower than the average of the three remaining factors at eight sites ($p < 0.031$). Hence, h should

Table 6. *p* values resulting from Method One for the runoff factors.[a]

Site	h	q_{max}	$h+q_{max}$	hq_{max}
Plot 4	0.32	0.19	**0.04**	***0.02***
Plot 2	**0.0005**	***0.007***	0.89	0.51
Plot 3	0.72	***0.031***	0.57	0.22
Plot 7	**0**	***4.9E-06***	0.84	***1.3E-06***
Plot 9	**0**	***1.5E-06***	0.96	***2.8E-05***
#3	**5.9E-09**	***1.7E-05***	0.10	***1.7E-03***
#4	**6.3E-07**	***1.3E-12***	**7E-10**	***5.0E-05***
#9	**4E-14**	***6.4E-15***	**3.8E-15**	***2.4E-14***
#12	**0.0006**	***2.9E-10***	**7.2E-05**	0.27

[a]Each p value corresponds to a Meng's Z_2 test and indicates whether the factor under examination is a contrast among the four runoff factors. Boldface denotes statistical significance at the 0.05 level. Non-italic boldface indicates a significantly higher correlation with *SSY* than the average of the three remaining factors. Italic boldface indicates a significantly lower correlation.

doi:10.1371/journal.pone.0117989.t006

be preferred to q_{max} as the predictive factor of *SSY*. The factor of $h+q_{max}$ is better correlated with *SSY* than the average of the three remaining factors at four sites ($p < 0.04$), whereas the factor of hq_{max} is less correlated with *SSY* than the average of the three remaining factors at six sites ($p < 0.02$). This demonstrates that the combination of q_{max} with h would impair rather than improve the ability of h to predict *SSY*.

Method Two—multiple Meng's Z_1 tests adjusted using the Hochberg approach

Meng's Z_2 tests used above have clearly demonstrated that T, I and P are inferior to other factors for application as the erosivity index. To reduce complexity, these factors are not considered in this section.

To test the significance of the difference between correlations of the nine rainfall factors of I_t, EI_t and PI_t with *SSY*, we performed 36 pairwise comparisons using Meng's Z_1 test at each of six sites within the Tuanshangou subwatershed. The resultant p values, together with the p' values after the Bonferroni correction, are presented in Table 7. Fifty-one among the 216 comparisons produced significant differences ($p < 0.05$) in the absence of the Bonferroni correction, with most (33) involving comparisons between PI_t and EI_t. When the Bonferroni correction was performed, significant differences remained for only 9 comparisons ($p' < 0.04$), all of which involved the comparison between PI_t and EI_t. The results adjusted using the Bonferroni correction demonstrate that EI_t is better correlated with *SSY* than PI_t in some cases, and the correlations with *SSY* was not significantly different among six factors of EI_t and I_t ($p' > 0.11$).

To compare the strength of correlations between *SSY* and the four runoff factors, we performed six Meng's Z_1 tests at each of nine sites within the Dalihe watershed. At seven sites, h is more correlated with *SSY* than q_{max} ($p < 0.001$, $p' < 0.01$; Table 8), regardless of whether the Bonferroni correction was applied. Only at Plot 4 was the obtained correlation coefficient between h and *SSY* smaller than that between q_{max} and *SSY* (Table 5). This difference, however, was not statistically significant ($p = 0.26$, $p' = 0.52$). A total of 18 comparisons at the nine sites were made between the correlations of h and the combined factors of h and q_{max} (i.e. $h+q_{max}$ and hq_{max}) with *SSY*. The Meng's Z_1 test suggested a significant difference for 11 among the 18 comparisons, and almost all (10) remain significant after the Bonferroni correction (Table 8). Among the ten comparisons, h is more correlated with *SSY* for nine ($p < 0.007$, $p' < 0.007$) and less correlated for only one ($p < 0.01$, $p' < 0.01$; #12). This again indicates that both q_{max} and its combination with h are inferior to the single factor of h for the *SSY* predictions.

Discussion

Rainfall factors

For rainfall factors, the results of two methods slightly differ: Method one suggested that I_{20}, I_{30}, EI_{10}, EI_{20} and EI_{30} are superior to other factors as a predictor of *SSY*; Method two excessively accepted I_{10} as an optimal predictor. This result may be related to the Bonferroni correction, which increases the likelihood of accepting the null hypothesis of identical correlations thereby increasing the risk of committing the type II errors [49].

The Loess Plateau is typically dominated by infiltration excess overland flows, and the runoff yield is determined by rainfall intensity rather than rainfall amount. In the Tuanshangou subwatershed, the median T is about 170 min. In contrast, the runoff duration at Plots 4, 2 and 3, with a median value of approximately 16 min, hardly exceeded 40 min. Rainfall during the low-intensity period is thus of little consequence to runoff yield and thus, to soil erosion. As a result, P is a poor indicator of *SSY*, as was also reported in [25, 40].

Table 7. *p* values resulting from Method Two for the rainfall factors.[a]

	Plot 4		Plot 2		Plot 3		Plot 7		Plot 9		#3	
	p	***p'***	***p***	***p'***	***p***	***p'***	***p***	***p'***	***p***	***p'***	***p***	***p'***
I_{10} vs. I_{20}	0.08	1.91	**0.04**	1.2	0.92	2.75	**0.02**	0.6	**0.04**	1.4	**0.02**	0.5
I_{30}	0.12	2.54	**0.04**	1.2	0.58	4.63	**0.02**	0.7	0.06	1.8	**0.03**	0.7
EI_{10}	0.20	3.48	0.29	4.9	0.82	4.10	0.09	2.8	**0.01**	0.5	**0.01**	0.4
EI_{20}	0.23	3.73	0.29	4.6	0.73	4.39	0.11	3.4	**0.04**	1.2	**0.02**	0.6
EI_{30}	0.47	5.64	0.45	5.8	0.38	4.53	0.17	4.8	0.09	2.3	0.05	1.3
PI_{10}	0.65	5.83	0.89	3.6	0.38	4.18	0.37	7.4	0.22	4.4	0.33	5.3
PI_{20}	0.67	4.70	0.95	0.9	0.22	3.93	0.41	7.8	0.31	4.1	0.33	5.6
PI_{30}	0.52	5.72	0.81	4.9	0.11	2.38	0.52	7.3	0.47	4.7	0.45	5.9
I_{20} vs. I_{30}	0.44	5.76	0.14	3.0	0.17	3.48	0.08	2.6	0.23	4.3	0.13	2.8
EI_{10}	0.65	6.46	0.95	1.9	0.83	3.33	0.53	6.9	0.09	2.3	0.15	2.9
EI_{20}	0.65	5.24	0.88	4.4	0.62	4.31	0.50	7.5	0.15	3.3	0.13	2.8
EI_{30}	0.97	1.94	0.90	2.7	0.25	4.05	0.60	7.2	0.31	4.4	0.26	5.0
PI_{10}	0.18	3.40	0.25	5.0	0.28	4.18	0.92	2.8	0.67	4.0	0.94	1.9
PI_{20}	0.19	3.46	0.29	4.4	0.12	2.62	0.92	3.7	0.81	3.2	0.99	1.0
PI_{30}	0.14	2.71	0.24	5.0	0.05	1.23	0.81	6.5	0.97	1.9	0.87	3.5
I_{30} vs. EI_{10}	0.87	3.47	0.53	6.4	0.37	4.79	0.80	7.2	0.23	4.2	0.43	6.0
EI_{20}	0.86	4.32	0.60	6.6	0.93	1.85	0.88	4.4	0.28	4.3	0.32	5.7
EI_{30}	0.72	4.31	0.44	6.1	0.43	4.30	0.86	6.0	0.50	4.0	0.50	4.5
PI_{10}	0.08	1.85	0.07	1.7	0.52	4.66	0.41	7.1	0.97	1.0	0.50	5.0
PI_{20}	0.08	1.78	0.08	1.8	0.22	3.79	0.41	7.4	0.82	2.5	0.56	3.9
PI_{30}	**0.05**	1.33	0.06	1.6	0.08	1.73	0.35	7.3	0.62	4.3	0.46	5.5
EI_{10} vs. EI_{20}	0.99	0.99	0.74	5.2	**0.01**	0.37	0.75	7.5	0.68	3.4	0.56	4.5
EI_{30}	0.28	4.16	0.65	6.5	**	0.11	0.94	1.9	0.48	4.4	0.94	2.8
PI_{10}	**	**	**0.01**	0.4	**0.01**	0.38	0.27	6.6	0.06	1.8	**0.02**	0.6
PI_{20}	**	**0.03**	**0.03**	0.9	**	0.07	0.32	7.1	0.07	1.8	0.06	1.5
PI_{30}	**	**0.03**	**0.03**	0.8	**	**0.02**	0.28	6.8	0.06	1.7	0.06	1.4
EI_{20} vs. EI_{30}	0.07	1.73	0.27	4.9	**	0.13	0.87	5.2	0.40	4.8	0.48	5.3
PI_{10}	**	**0.01**	**0.02**	0.5	0.19	3.62	0.21	5.6	0.09	2.3	**0.01**	0.3
PI_{20}	**	**	**0.01**	0.4	**0.01**	0.38	0.18	5.1	**0.04**	1.3	**0.01**	0.4
PI_{30}	**	**	**	0.2	**	**0.04**	0.15	4.4	**0.03**	1.0	**0.01**	0.4
EI_{30} vs. PI_{10}	**0.01**	0.31	0.07	1.7	0.95	0.95	0.29	6.8	0.28	4.5	**0.04**	1.2
PI_{20}	**	0.11	**0.05**	1.3	0.31	4.32	0.21	5.4	0.10	2.3	**0.03**	0.8
PI_{30}	**	**	**	0.3	**0.01**	0.36	0.09	2.9	**0.02**	0.8	**0.01**	0.2
PI_{10} vs. PI_{20}	0.93	2.78	0.71	5.7	**0.02**	0.56	0.97	1.0	0.47	5.1	0.71	4.3
PI_{30}	0.38	5.39	0.68	6.2	**	0.13	0.67	7.3	0.26	4.5	0.78	3.9
PI_{20} vs. PI_{30}	0.10	2.30	0.26	5.0	**	0.13	0.46	7.4	0.20	4.3	0.38	5.7

[a] Each *p* value represents a paired comparison using Meng's Z_1 test. The *p'* values represent those adapted using the Hochberg approach [47].

** indicates statistically significant differences at the 0.01 level. Boldface indicates statistically significant differences at the 0.05 level.

doi:10.1371/journal.pone.0117989.t007

The single factor of I_{30}, although equally as effective in predicting *SSY* as factors of I_{20}, EI_{10}, EI_{20} and EI_{30}, can be preferentially used as the rainfall erosivity index in practices because I_{30} is in form simpler than EI_t and can be measured somewhat more accurately than I_{20}. *Wang* [16] also noted that the predictive ability of EI_t is only marginally higher than that of I_t in the Loess Plateau. The calculation of *E* involves data which are rarely available. Our finding shows that *E*

Table 8. *p* values resulting from Method Two for the runoff factors.[a]

		Plot 4		Plot 2		Plot 3		Plot 7		Plot 9	
		p	***p'***	***p***	***p'***	***p***	***p'***	***p***	***p'***	***p***	***p'***
h	*vs.* q_{max}	0.26	0.52	**	**	0.15	0.61	**	**	**	**
	$h+q_{max}$	0.09	0.34	0.05	0.15	0.90	0.90	**	**	**	**
	hq_{max}	0.49	0.49	**0.01**	0.05	0.62	1.87	**	**	**	**
		#3		**#4**		**#9**		**#12**			
		P	***p'***	***p***	***p'***	***p***	***p'***	***p***	***p'***		
h	*vs.* q_{max}	**	**	**	**	**	**	**	**		
	$h+q_{max}$	**	**	0.47	0.47	0.77	1.54	** [b]	** [b]		
	hq_{max}	**	**	**	**	**	**	**	**		

[a] *p* values directly result from Meng's Z_1 test and *p'* values are corrected values using the Hochberg approach [47].

** indicates statistically significant differences at the 0.01 level. Boldface indicates statistically significant differences at the 0.05 level.

[b] This test suggests that *h* is less correlated with *SSY* than $h+q_{max}$ although the obtained correlated coefficients are almost the same (0.973 vs 0.975). Other significant results all suggest a stronger correlation for *h*.

doi:10.1371/journal.pone.0117989.t008

is not necessarily included into the rainfall erosivity index thereby facilitating the obtainment of rainfall erosivity in the Loess Plateau.

Our calculations at six sites within the Tuanshangou subwatershed indicate that I_{30} summed over a year can explain 71 to 89% of the variation in yearly soil loss, an accuracy that is

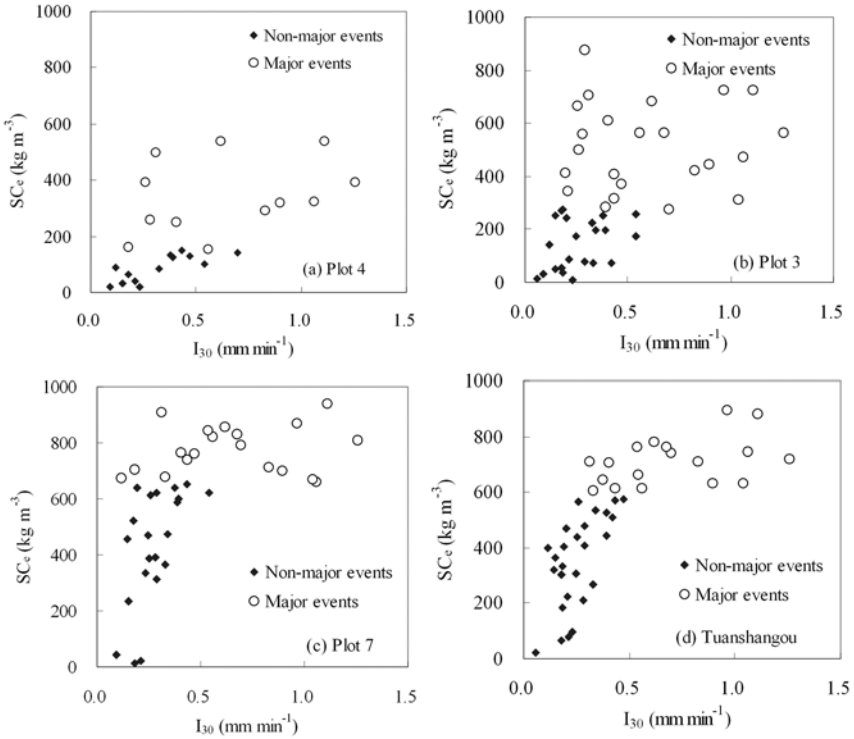

Fig 2. The relationship between I_{30} and SC_e for the Tuanshangou station (#3) and three experimental runoff plots within it.

doi:10.1371/journal.pone.0117989.g002

comparable to that of the use of the EI_{30} index in the USA [40]. Considering the fact that our data are from cropped plots, I_{30} can be directly applied to predicting soil loss in cropped areas, as opposed to the USLE, which first predicts erosion for the unit plot (bare fallow areas 22.1 m long on a 9% slope) and then predicts for the area of interest by introducing the topographic factors and the cover and management factors. Nevertheless, the mean of the annual cumulative I_{30} promises to act as the R factor of the USLE due to the sparse vegetation cover in the plots.

Runoff factors

For runoff factors, the two methods present the same result: h is not only superior to q_{max} but is also superior to the combined factors of h and q_{max} as a predictor of SSY.

Similar to the rainfall case, flow discharge during flood events is primarily concentrated during the high-flow period, especially during the peak-flow period. Consequently, q_{max} correlates well with h ($r > 0.77$) and in turn, with SSY at every site ($r > 0.83$, Table 5). However, sediment concentrations at moderate discharges are more or less the same as those at high discharges in the Loess Plateau. Extremely high concentrations even primarily occur at low discharges from plots to watersheds (see Fig. 6 in [44] and Fig. 2 in [34]). This mismatch between sediment concentration and water discharge can be related to hyperconcentrated flows, which are well developed from upland slopes to river channels in the Loess Plateau [50, 51]. It is known that no direct relationship exists between sediment concentration and water discharge for hyperconcentrated flows [52]. In stream channels of the Chabagou watershed (#9), SC_{max} generally occur at flow discharges that are approximately 30–50% lower than q_{max} [53]. Hence, contrary to the rainfall case, h is more correlated with SSY than q_{max}.

Runoff factors can provide better SSY predictions than rainfall factors in the Loess Plateau in terms of correlations (See Tables 3 and 5). The obtained correlation coefficients between h and SSY is larger than those between I_{30} and SSY at all six sites within the Tuanshangou subwatershed, and five of them being statistically valid ($p < 0.02$). Interrill erosion is closely related to rainfall factors, whereas rill erosion is primarily dependent on runoff factors [25, 54]. The higher correlation of runoff factors with SSY relative to rainfall factors can thus be linked to the dominance of rill erosion and the mass wasting over the interrill erosion in our study area.

The best erosivity index

The rainfall-runoff factors we examined are generally inter-correlated. As a result, it can hardly be expected to improve the prediction accuracy by introducing more factors. SSY equals the product of h and SC_e. There is no need to include factors that do not affect SC_e into the erosivity index if h has been included. We hereafter examine the correlations between the rainfall-runoff factors and SC_e.

Except for T, I and P, nine other rainfall factors correlate well with SC_e at all sites ($p < 0.01$). However, almost all of these correlations become insignificant with only two exceptions when only major sediment-producing events are considered (see Table 3). As in [35], we defined major sediment-producing events as high-concentrated events that accumulatively contribute 90% to the total sediment yield of all examined events. Scatter plots of SC_e and I_{30} at all sites are generally parallel to the x-axis for major sediment-producing events (Fig. 2), a result contrary to that observed by *Kinnel* [29] and *Chaplot et al.* [55]. The same observation holds for scatter plots of SC_{max} and I_{30} (Fig. 3).

For major sediment-producing events, SC_e and SC_{max} also remain independent of the four runoff factors although there are five exceptions among the 36 derived correlations (Table 5). Fig. 4 and Fig. 5 depict the relationships between SC_e and q_{max} and between SC_{max} and q_{max}, respectively.

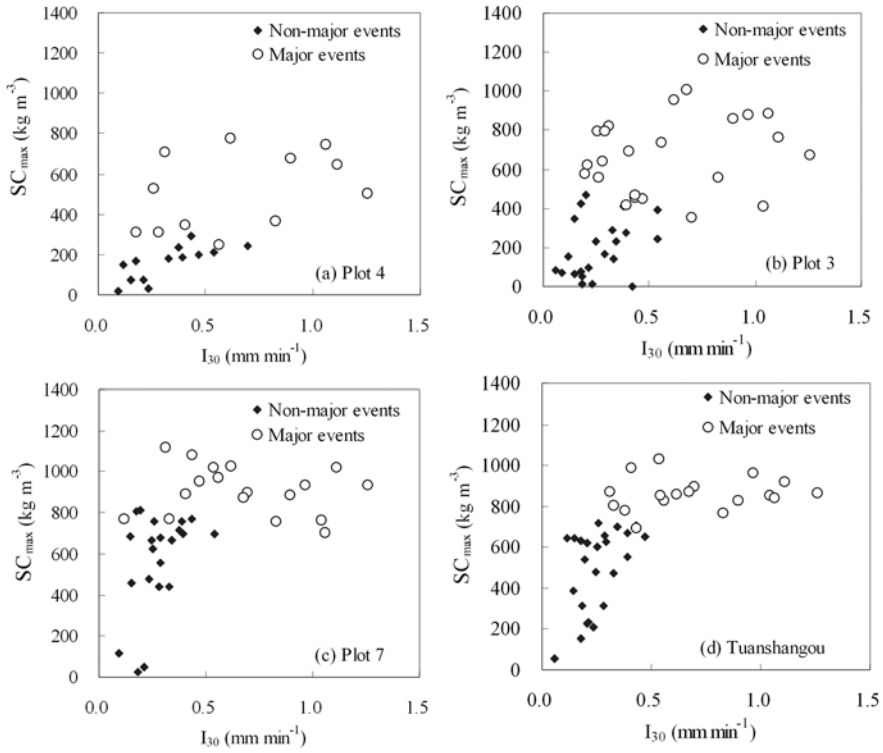

Fig 3. The relationship between I_{30} and SC_{max} for the Tuanshangou station (#3) and three experimental runoff plots within it.

doi:10.1371/journal.pone.0117989.g003

In terms of the correlation with *SSY*, the single factor of *h* is the best erosivity index among factors we examined at scales from plots to watersheds. It is not expected that the prediction accuracy would be further improved by introducing additional rainfall-runoff factors because these factors are ineffective in altering SC_e for major sediment-producing events. As was the case of q_{max}, little was added to the prediction accuracy by combining *h* with I_{30}. Among the six sites within the Tuanshangou subwatershed, $h+I_{30}$ performs better than *h* only at one site ($p = 0.03$; Table 9), and hI_{30} is not as good as *h* at three sits ($p < 0.046$). When the runoff coefficient (*a*, given by *h* divided by *P*) was introduced, as did in the USLE-M [27], neither aI_{30} nor aEI_{30} provide better predictions of *SSY* than *h* at any site in terms of correlations. Moreover, aI_{30} and aEI_{30} are less correlated with *SSY* than *h* at three and two sites, respectively ($p < 0.006$; Table 9).

Conclusions

Based on Meng's tests, this study presents two methods to determine the erosivity index among a number of rainfall-runoff factors by comparing their correlations with *SSY*. The first method involves a stepwise procedure to remove factors that are poorly correlated with *SSY*. The second method involves multiple comparisons that are adjusted using a Bonferroni correction. It appears that few studies have compared correlations on a statistical basis, not only within the soil erosion community but also within the entire geoscience community. Our methods therefore have wide significance, not only for determining the best predictor, but also in other respects, such as comparing model performance, which is often indexed by the correlation between observed and modeled values.

Using the methods described above, we determined the erosivity indices of rainfall and runoff in a typical Chinese Loess Plateau watershed. Among 12 rainfall factors under examination,

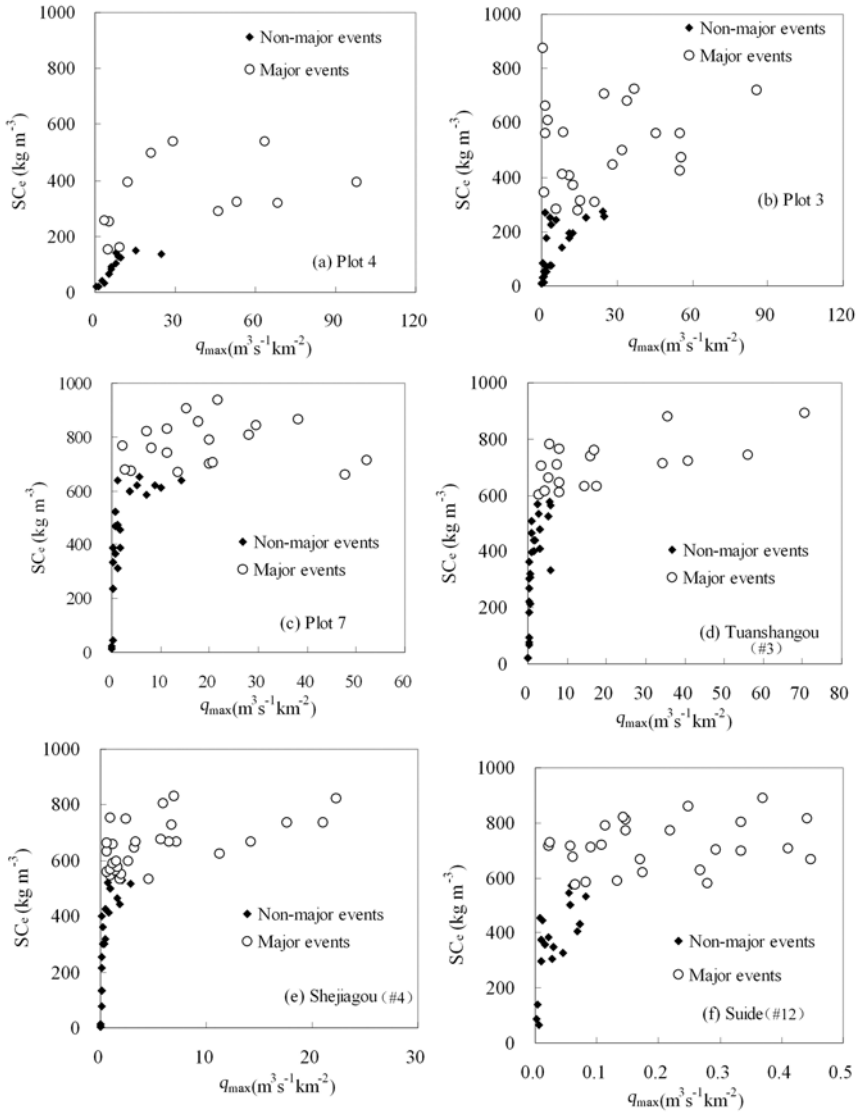

Fig 4. The relationship between q_{max} and SC_e for plots and watersheds within the Dalihe watershed

doi:10.1371/journal.pone.0117989.g004

I_{20}, I_{30}, EI_{10}, EI_{20} and EI_{30} were found to be the most correlated with *SSY* at scales from plots to subwatersheds (< 1 km^2). We suggested the use of I_{30} as the rainfall erosivity index, although it is equally effective as the three remaining factors. The value of I_{30} summed over one year is also a good predictor of annual soil loss ($r^2 > 0.7$).

Runoff factors are more correlated with SSY than rainfall factors almost at all examined sites. Among the four studied runoff factors, h is correlated best with SSY at scales from plots to watersheds. Moreover, the combination of h with other rainfall-runoff factors, including rainfall intensity and peak discharge (as used in the MUSLE [24]), does not show enhanced ability to predict SSY compared with the single factor of h because these factors are of little importance in determining sediment concentration for major sediment-producing events. Introducing the runoff coefficient (as used in the USLE-M [27]) also added little to the prediction accuracy. Hence, we considered the single factor of h as the best erosivity index, although I30 would be useful in many cases considering the difficulty of measuring runoff.

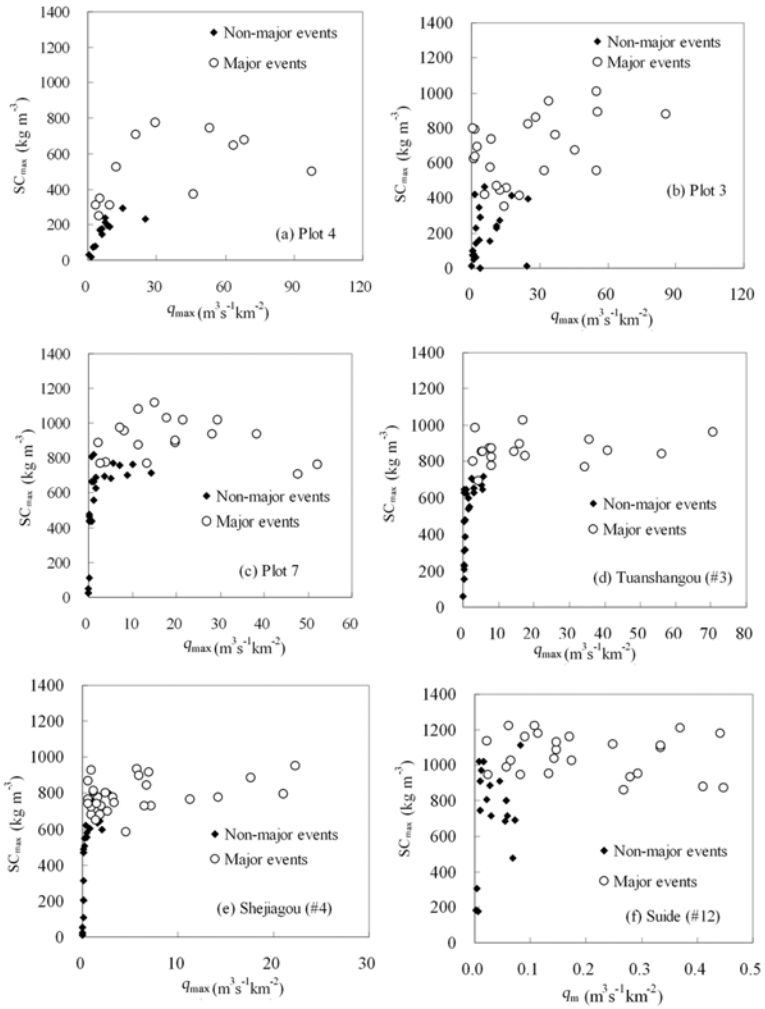

Fig 5. The relationship between q_{max} and SC_{max} for plots and watersheds within the Dalihe watershed.

doi:10.1371/journal.pone.0117989.g005

Table 9. Correlation coefficients between some combined factors and *SSY* and the comparisons with those between *h* and SSY.[a]

Site	correlation coefficients				*p* [a]			
	$h+I_{30}$	hI_{30}	aI_{30} [b]	aEI_{30} [b]	$h+I_{30}$	hI_{30}	aI_{30} [b]	aEI_{30} [b]
Plot 4	0.94	0.95	0.93	0.95	0.26	0.58	0.67	0.42
Plot 2	0.96	0.94	0.93	0.94	0.22	0.22	0.11	0.16
Plot 3	0.95	0.94	0.95	0.94	0.41	0.76	0.80	0.95
Plot 7	0.99	0.96	0.94	0.95	**0.03**	***5E-07***	***3E-10***	***3E-08***
Plot 9	0.99	0.98	0.96	0.98	0.40	***0.006***	***4E-07***	***0.006***
#3	0.99	0.98	0.97	0.98	0.07	***0.046***	***0.002***	0.08

[a] *p* values result from Meng's Z_1 test. Each *p* value represents a comparison between correlations of a combined factor and *h* with *SSY*. Boldface denotes statistical significance at the 0.05 level. Non-italic Boldface indicates that the combined factor is more correlated with *SSY* than *h*, whereas italic boldface indicates the combined factor is less correlated with *SSY* than *h*.

[b] *a*, the runoff coefficient, is computed by dividing *h* by *P*.

doi:10.1371/journal.pone.0117989.t009

Acknowledgments

We appreciate the suggestions of the anonymous reviewer and the editor. Thanks to the Data Sharing Infrastructure of Earth System Science-Data Sharing Infrastructure of Loess Plateau for providing our data.

Author Contributions

Conceived and designed the experiments: MGZ. Performed the experiments: MGZ XAC. Analyzed the data: MGZ. Contributed reagents/materials/analysis tools: MGZ XAC. Wrote the paper: MGZ.

References

1. Angulo-Martínez M, Beguería S (2009) Estimating rainfall erosivity from daily precipitation records: A comparison among methods using data from the Ebro Basin (NE Spain). J Hydrol 379:111–121. doi: 10.1016/j.jhydrol.2009.09.051.
2. Lee J-H, Heo J-H (2011) Evaluation of estimation methods for rainfall erosivity based on annual precipitation in Korea. J Hydrol 409: 30–48. doi: 10.1016/j.jhydrol.2011.07.031.
3. Shi ZH, Cai CF, Ding SW, Wang TW, Chow TL (2004) Soil conservation planning at the small watershed level using RUSLE with GIS: a case study in the Three Gorge Area of China. Catena 55: 33–48. doi: 10.1016/S0341-8162(03)00088-2.
4. Wischmeier WH, Smith DD (1978) Predicting rainfall erosion losses: a guide to conservation planning. USDA Handbook 537, Washington, DC.
5. Renard KG, Foster GR, Weesies GA, McCool DK, Yoder DC (1997) Predicting soil erosion by water: a guide to conservation planning with the revised universal soil loss equation (RUSLE). USDA Handbook 703, Washington, DC.
6. Yue BJ, Shi ZH, Fang NF (2014) Evaluation of rainfall erosivity and its temporal variation in the Yanhe River Catchment of the Chinese Loess Plateau. Natural Hazards 74:585–602. doi: 10.1007/s11069-014-1199-z.
7. Diodato N, Bellocchi G (2007) Estimating monthly (R)USLE climate input in a Mediterranean region using limited data. J Hydrol 345:224–236. doi: 10.1016/j.jhydrol.2007.08.008.
8. Hudson N (1971) Soil Conservation. Ithaca: Cornell University Press.
9. Lal R (1976) Soil erosion on Alfisols in Western Nigeria, III-Effects of rainfall characteristics. Geoderma 16: 389–401. doi: 10.1016/0016-7061(76)90003-3.
10. Kinnell PIA (1995) The I_xE_A erosivity index: An index with the capacity to give more direct consideration to hydrology in predicting short-term erosion in the USLE modeling environment. J Soil Water Conserv 50: 507–512.
11. Sukhanovski YP, Ollesch G, Khan KY, Meißner R (2001) A new index for rainfall erosivity on a physical basis. Journal of Plant Nutrition and Soil Science 65 (1), 51–57.
12. Sinzot A, Bollinne A, Laurant A, Erpicum M, Pissart A (1989) A contribution to the development of an erosivity index adapted to the prediction of erosion in Belgium. Earth Surf Process Landf 14: 509–515. doi: 10.1002/esp.3290140607.
13. Usón A, Ramos MC (2001) An improved rainfall erosivity index obtained from experimental interrill soil losses in soils with a Mediterranean climate. Catena 43: 293–305. doi: 10.1016/S0341-8162(00)00150-8.
14. Abu Hammad AH, Borresen T, Haugen LE (2005) Effects of rain characteristics and terracing on runoff and erosion under the Mediterranean. Soil Tillage Res 87 39–47. doi: 10.1016/j.still.2005.02.037.
15. Sharifah Mastura SA, Al-Toum S, Jaafar O (2003) Rainsplash erosion: a case study in Tekala River catchment, East Selangor, Malaysia. Geografia 4: 44–59.
16. Wang WZ (1983) Relationship between soil loss and rainfall characteristics for the Chinese loess areas. Bull Soil Water Conserv (5:): 62–64. (in Chinese)
17. Jia ZJ, Wang XP, Li JY (1987) Determination of the rainfall erosivity index for hilly loess areas in the western Shanxi. Soil Water Conserv Chin (6:):18–20. (in Chinese)
18. Wang WZ (1987) Determination of the rainfall erosivity index for Chinese loess areas. Soil Water Conserv Chin (12:): 34–38. (in Chinese)
19. Chen XA, Cai QG, Zheng MG, Nie BB, Cui PW (2010) Study on rainfall erosivity of Chabagou watershed in a hilly loess region on the Loess Plateau. J Sediment Res (1:): 5–10. (in Chinese)

20. Jia Z, Jiang ZS, Liu Z (1990) Studies of the relationship between rainfall characteristics and soil loss. Memoir of NISWC, Academia Sinica & Ministry of Water Conservancy 12: 9–15. (in Chinese).
21. Wang WZ, Jiao JY (1996a) A quantitive study of soil erosion factors in China. Bull Soil Water Conserv 16(5): 1–20. (in Chinese)
22. Shi ZH, Yue BJ, Wang L, Fang NF, Wang D, Wu FZ (2013) Effects of mulch cover rate on interrill erosion processes and the size selectivity of eroded sediment on steep slopes. Soil Sci Soc Am J 77: 257–267. doi: 10.2136/sssaj2012.0273.
23. Dragoun FJ (1962) Rainfall energy as related to sediment yield. J Geophys. Res 67:1495–1501. doi: 10.1029/JZ067i004p01495.
24. Williams JR (1975) Sediment-yield prediction with universal equation using runoff energy factor. In: Present and Prospective Technology for Predicting Sediment Yield and Sources, Publ. ARS-S-40. US Dept. Agric., Washington, DC, pp. 244–252.
25. Foster GR, Lambaradi F, Moldenhauer WC (1982) Evaluation of rainfall-runoff erosivity factors for individual storms. Trans Am Soc Agric Eng 25:124–129.
26. Hussein MH, Awad MM, Abdul-Jabbar AS (1994) Predicting rainfall-runoff erosivity for single storms in northern Iraq. Hydrol Sci J 39:535–547. doi: 10.1080/02626669409492773.
27. Kinnell PIA, Risse LM (1998) USLE-M: empirical modelling rainfall erosion through runoff and sediment concentration. Soil Sci Soc Am J 62: 1667–1672. doi: 10.2136/sssaj1998.03615995006200060026x.
28. Williams JW, Izaurralde RC, Steglich EM (2008) Agricultural Policy/Environmental Extender Model Theoretical Documentation. BRC Report # 2008–17. Blackland Research and Extension Center, Temple, Texas.
29. Kinnell PIA (2010) Event soil loss, runoff and the Universal Soil Loss Equation family of models: A review. J Hydrol 385: 384–397. doi: 10.1016/j.jhydrol.2010.01.024.
30. Mou JZ, Xiong GS (1980) Prediction of sediment yield and calculation of trapped sediment by soil conservation measures from small catchments in Northern Shaanxi, China. In: Proceedings of the First International Symposium on River Sedimentation. Beijing: Guanghua Press, pp. 73–82 (in Chinese).
31. Cai QG, Liu JG, Liu QJ (2004) Research of sediment yield statistical model for single rainstorm in Chabagou drainage basin. Geog Res 23(4): 433–439. (in Chinese)
32. Yu GQ, Zhang MS, Li ZB, Li P, Zhang X, Cheng SD (2013) Piecewise prediction model for watershed-scale erosion and sediment yield of individual rainfall events on the Loess Plateau, China. Hydrol Process. doi: 10.1002/hyp.10020.
33. Wang ML, Zhang R (1990) Study on sediment yield model under single storm in Chabagou watershed. J Soil Water Conserv 4 (1): 11–18. (in Chinese)
34. Zheng MG, Cai QG, Cheng QJ (2008) Modelling the runoff-sediment yield relationship using a proportional function in hilly areas of the Loess Plateau, North China. Geomorphology 93: 288–301. doi: 10.1016/j.geomorph.2007.03.001.
35. Zheng MG, Yang JS, Qi DL, Sun LY, Cai QG (2012) Flow-sediment relationship as functions of spatial and temporal scales in hilly areas of the Chinese Loess Plateau. Catena 98: 29–40. doi: 10.1016/j.catena.2012.05.013.
36. Salako F, Obi ME, Lal R (1991) Comparative assessment of several rainfall erosivity indices in Southern Nigeria. Soil Technol 4,: 93–97. doi: 10.1016/0933-3630(91)90042-L.
37. Kiassari EM, Nikkami D, Mahdian MH, Pazira E (2012) Investigating rainfall erosivity indices in arid and semiarid climates of Iran. Turk J Agric For 36: 365–378.
38. Wischmeier WH, Smith DD (1958) Rainfall energy and its relationship to soil loss. Trans. Am. Geophys. Union, 392, 285–291. doi: 10.1029/TR039i002p00285.
39. Wischmeier WH, Smith DD, Uhland RE (1958) Evaluation of factors in the soil loss equation. Agric Eng 39: 458–462.
40. Wischmeier WH (1959) A rainfall erosion index for a universal soil-loss equation. Soil Sci Soc Am J 23: 246–249. doi: 10.2136/sssaj1959.03615995002300030027x.
41. Silver NC, Hittner JB, May K (2006) A FORTRAN 77 program for comparing dependent correlations. Appl Psychol Meas 30(2): 152–153. doi: 10.1177/0146621605277132.
42. Meng XL, Rosenthal R, Rubin DB (1992) Comparing correlated correlation coefficients. Psychol Bull 111: 172–175. doi: 10.1037/0033-2909.111.1.172.
43. Zheng MG, Qin F, Sun LY, Qi DL, Cai QG (2011) Spatial scale effects on sediment concentration in runoff during flood events for hilly areas of the Loess Plateau, China. Earth Surf Processes Landforms 36: 1499–1509. doi: 10.1002/esp.2176.

44. Zheng MG, Qin F, Yang JS, Cai QG (2013) The spatio-temporal invariability of sediment concentration and the flow-sediment relationship for hilly areas of the Chinese Loess Plateau. Catena 109: 164–176. doi: 10.1016/j.catena.2013.03.017.

45. Jiang ZS, Song WJ, Li XY (1983) Studies of the raindrop characteristics for Chinese loess area. Soil Water Conserv Chin (3:): 32–36. (in Chinese)

46. Goyal JK, Sharma JN (2009) Mathematical Statics. Meerut: Krishna Prakashan Media (P) Ltd., 464pp.

47. Hochberg Y (1988) A sharper Bonferroni procedure for multiple tests of significance. Biometrika 75: 800–802. doi: 10.1093/biomet/75.4.800.

48. Wright SP (1992) Adjusted P-Values for Simultaneous Inference. Biometrics, 48: 1005–1013.

49. Rice TK, Schork NJ, Rao DC (2008) Methods for handling multiple testing. Adv Genet 60: 293–308. doi: 10.1016/S0065-2660(07)00412-9 PMID: 18358325

50. Xu JX (1999) Erosion caused by hyperconcentrated flow on the Loess Plateau. Catena 36: 1–19. doi: 10.1016/S0341-8162(99)00009-0.

51. Liu QJ, Shi ZH, Fang NF, Zhu HD, Ai L (2013) Modeling the daily suspended sediment concentration in a hyperconcentrated river on the Loess Plateau, China, using the Wavelet-ANN approach. Geomorphology 186: 181–190. doi: 10.1016/j.geomorph.2013.01.012.

52. Pierson TC (2005) Hyperconcentrated flow-transitional process between water flow and debris flow. In: Jakob M, Hungr O, editors. Debris-Flow Hazards and Related Phenomena. Berlin Heidelberg: Springer, pp. 159–202.

53. Wang WZ, Jiao JY (1996b) Statistic analysis on process of gully runoff and sediment yield under different rain pattern in loess plateau region. Bull. Soil Water Conserv 16 (6): 12–18 (in Chinese).

54. Shi ZH, Fang NF, Wu FZ, Wang L, Yue BJ, Wu GL (2012) Soil erosion processes and sediment sorting associated with transport mechanisms on steep slopes. J Hydrol 454: 123–130. doi: 10.1016/j.jhydrol.2012.06.004.

55. Chaplot VAM, Le Bissonnais Y (2003) Runoff features for interrill erosion at different rainfall intensities, slope lengths, and gradients in an agricultural loessial hillslope. Soil Sci Soc Am J 67: 844–851. doi: 10.2136/sssaj2003.8440.